

**SA53A-2525**

**Kenneth R Bromund<sup>1</sup>, Guan Le<sup>1</sup>, Todd M Bonalsky<sup>1</sup>, Matthew Finley<sup>2</sup>, Eftyhia Zesta<sup>1</sup>, Rodolfo Wottrich<sup>3</sup>, Marcelo Banik de Pádua<sup>4</sup>, Charles Swenson<sup>5</sup>, Roderick A Heelis<sup>6</sup>, Linda Habash Krause<sup>7</sup>, Luis Loures<sup>3</sup> and Lidia Sato<sup>3</sup>**

(1) NASA Goddard Space Flight Center, Greenbelt, MD, United States  
 (2) University of Maryland, College Park, NASA/GSFC, Greenbelt, MD, United States  
 (3)ITA Technological Institute of Aeronautics, Sao Jose dos Campos, Brazil  
 (4)INPE National Institute for Space Research, Sao Jose dos Campos, Brazil

(5) Utah State University, Department of Electrical and Computer Engineering, Logan, UT, United States  
 (6) University Texas Dallas, Richardson, TX, United States  
 (7) NASA Marshall Space Flight Ctr, Huntsville, AL, United States

For more information, contact [kenneth.r.bromund@nasa.gov](mailto:kenneth.r.bromund@nasa.gov)

## Background

The Scintillation Prediction Observations Research Task (SPORT) is a 6U CubeSat mission designed to study the conditions under which ionospheric variability develops at low latitudes. SPORT is an international partnership between NASA, the Brazilian National Institute for Space Research (INPE), and the Technical Aeronautics Institute under the Brazilian Air Force Command Department (DCTA/ITA), with the Brazilian partners contributing the spacecraft, observatory integration and test, mission operations and data management [Spann, et al., 2017].

Payloads:

- Space Weather Probe (SPW) including a Langmuir probe, Impedance Probe and Electric Fields Probes, Utah State University
- Ion Velocity Meter (IVM), University of Texas Dallas
- Miniaturized Science Magnetometer (MSM), NASA Goddard Space Flight Center
- Compact Total Electron Content Sensor (CTECS), Aerospace Corporation.

## The MSM Instrument

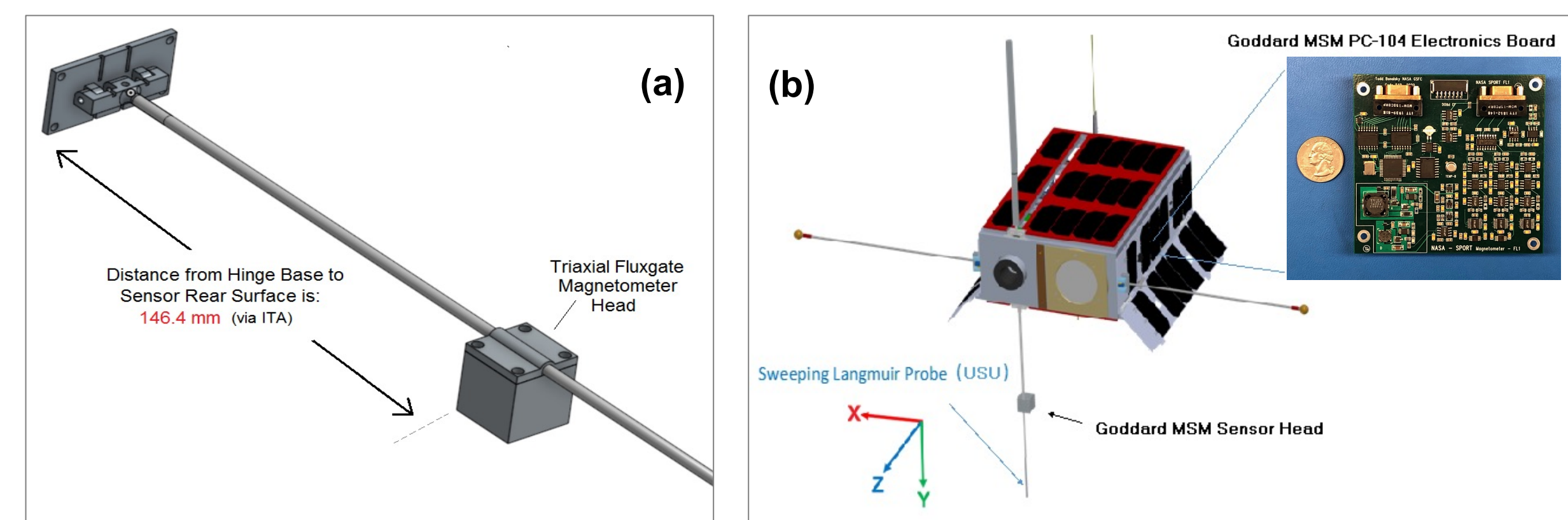
Instrument Requirement:

- ± 56,000 nT dynamic range
- ± 100 nT precision
- ± 100 nT accuracy
- 1 km along-track sampling

Instrument Performance:

- ± 65,000 nT dynamic range
- 7.7 pT/bit resolution
- 10 Hz sample rate

**Fig. 1 (a)** GSFC provided the 30 cm boom on which MSM is mounted 15 cm away from the bus, as well as the hinge assembly. **(b)** The location of the MSM fluxgate sensor and electronics board on the SPORT spacecraft, and the orientation of the MSM sensor axes. The Langmuir probe is mounted at the end of the MSM boom.



## Mission Operations/Data Coverage

SPORT was deployed into a low Earth orbit from the International Space Station on December 29, 2022. Science measurements are available from the time of MSM boom deployment on May 12, 2023, through September 23, 2023 before re-entry of the SPORT satellite in early October 2023.

While the mission was designed for ram-point 3-axis stabilized attitude control, SPORT remained in a 'controlled tumble' state for the duration of the mission, and the star camera was operational for a limited subset of the available MSM measurements, as shown in Fig. 2.

Most science operations are between dusk and dawn in the latitude range +/-40°, with occasional excursions to +/- 50°.

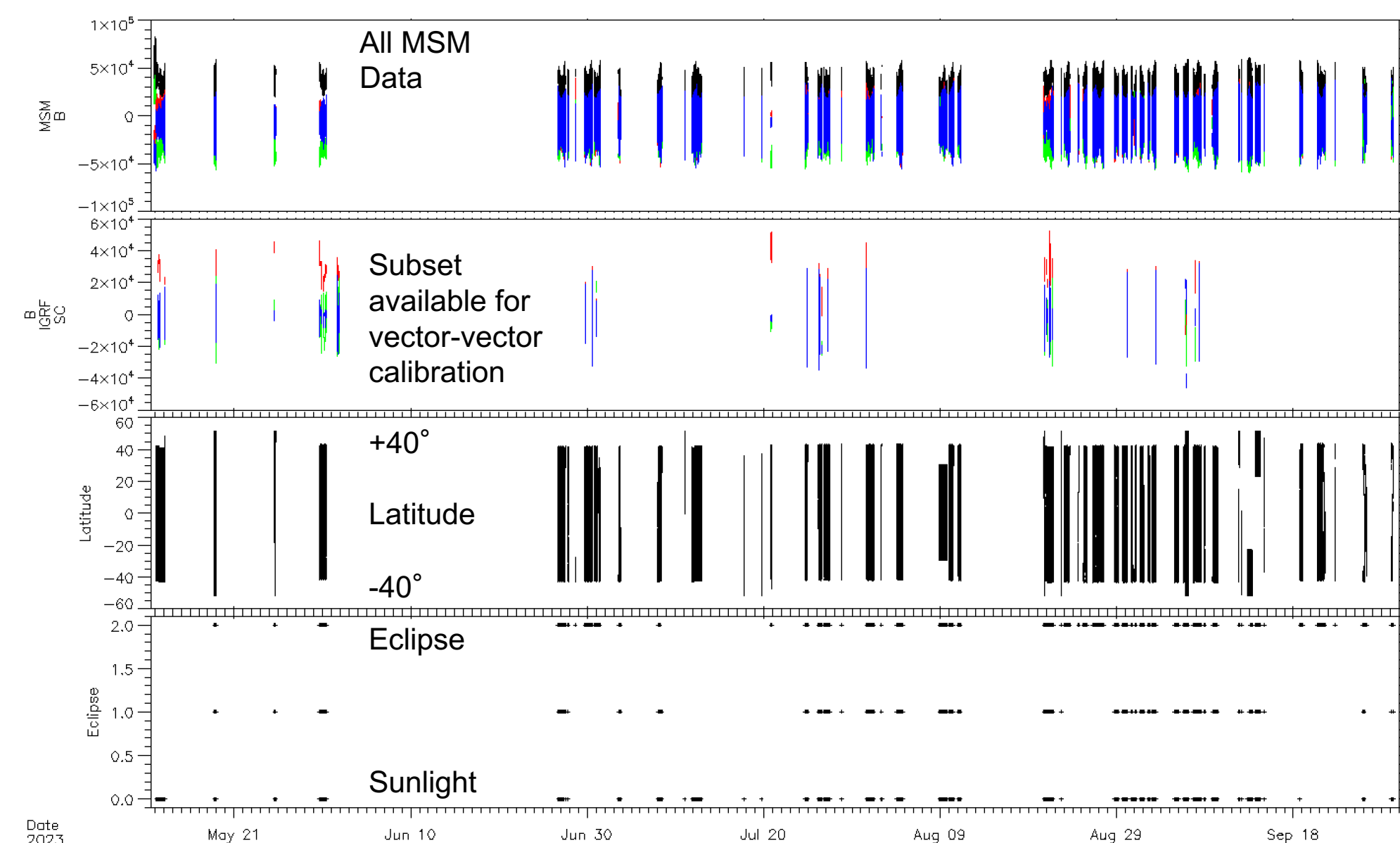


**Fig. 2:** Data Coverage for MSM and the star camera for the entire SPORT mission. The lower panels show coverage with respect to latitude and sunlight vs eclipse.

## On-Orbit Calibration

### Orthogonalization

The measurement on each MSM sensor axis,  $E_i$  (in pseudo-nT) is related to the ambient magnetic field,  $\mathbf{B} = (B_x, B_y, B_z)^T$  (in nT) in the SC reference frame, by the elements of an orthogonality matrix,  $m_{ij}$  and a magnetic offset  $o_i$  (in pseudo-nT). We solve for the non-orthogonality and offsets by tri-linear regression on each axis,  $i$ :

$$E_i = m_{i1}B_x + m_{i2}B_y + m_{i3}B_z + o_i$$

Due to the tumbling motion of the spacecraft, the relative orientations of the sensor triad to the ambient field cover nearly  $4\pi$  steradians, and the magnetic field strength on each sensor axis covers a sufficient portion of the dynamic range to obtain an estimate of each element of the orthogonality matrix, as shown below in Fig. 3.

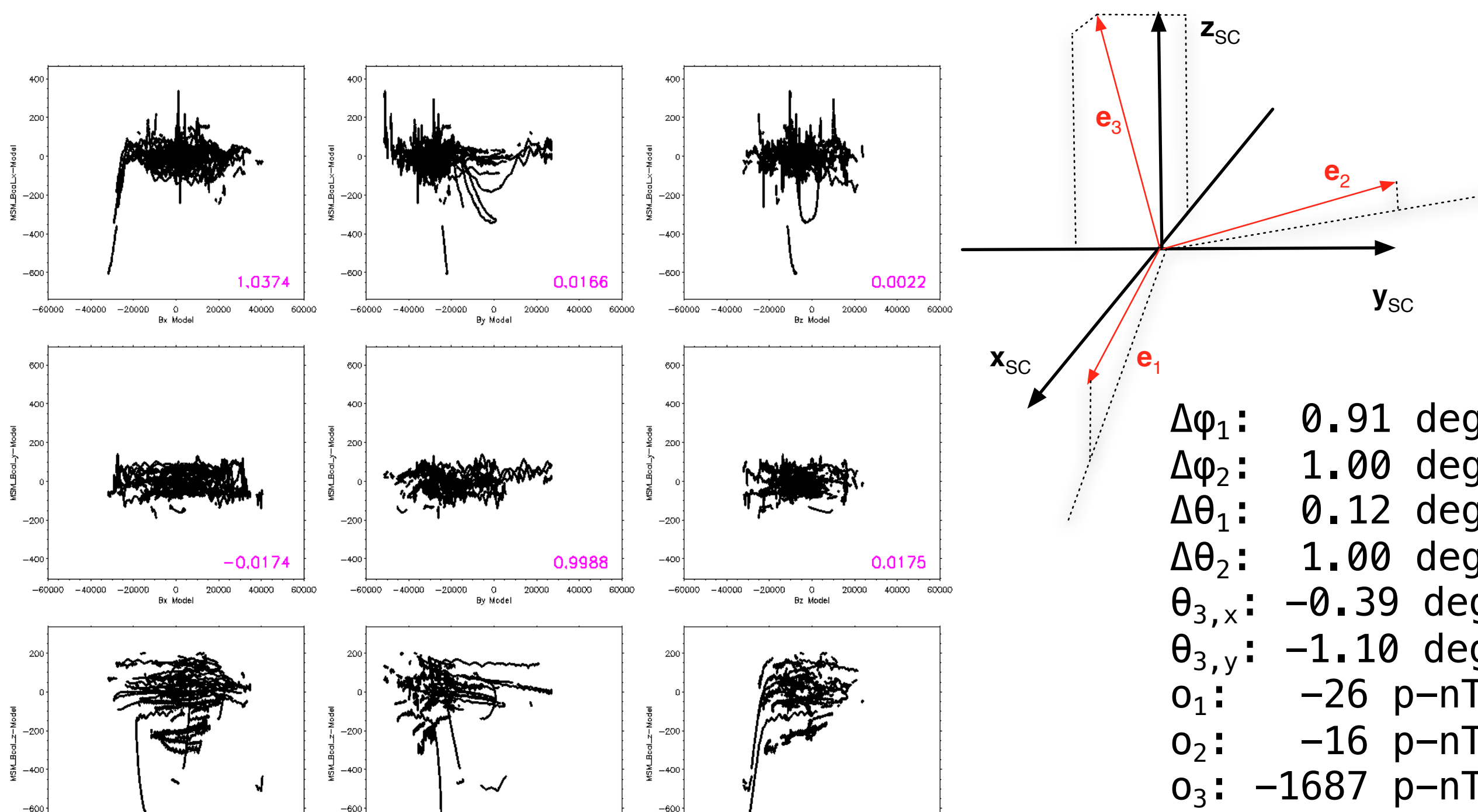


**Fig. 3:** Non-orthogonality Matrix

### Nonlinearity

There is a strong non-linearity in the scale factors. It was essential to apply a non-linearity correction to the Y-axis before performing the orthogonalization shown above, because the non-linearity effectively causes an offset shift of 2000 nT over the dynamic range of the sensor. On-orbit analysis shows that the gain is piecewise linear. A non-linearity correction is constructed by splining together linear fits to the gain determined over limited ranges of the raw  $E_2$  output, as shown below:

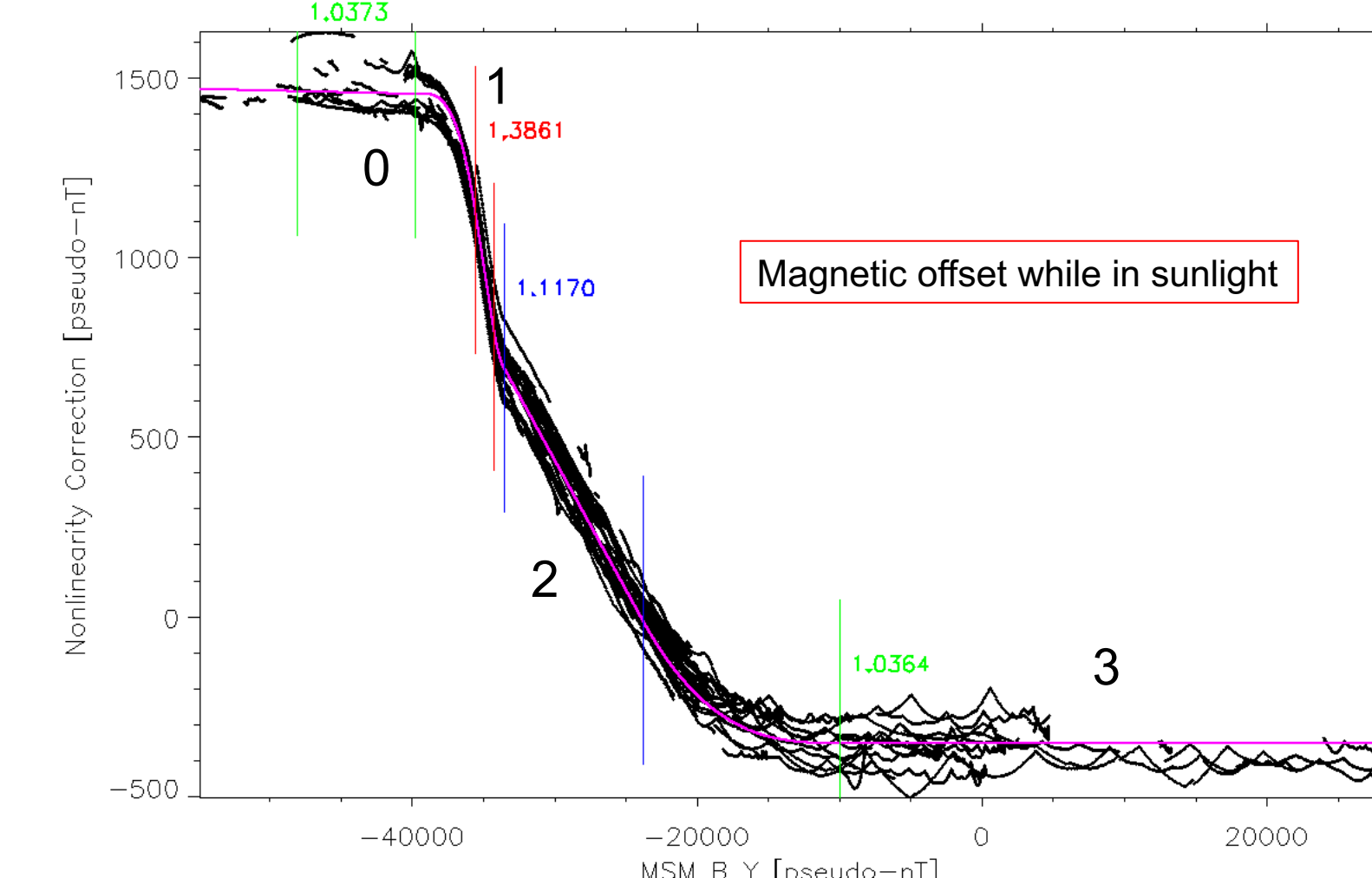


**Fig. 4:** Y-axis nonlinearity. There are 4 field ranges where the response is linear. Residual effect are worst in the transitions, and in region 1, which is the steepest.

For the X- and Z- axes, the orthogonalization was performed by limiting the range of  $B_x > -23000$  and  $B_y > -17000$  nT to avoid non-linearities. The non-linearities in these ranges are visible in the non-orthogonality matrix plot (Fig. 3) above, but the availability of star-camera solutions limits the range on which the non-linearities can be fully characterized. Residual non-linearity in stronger fields is observed by inspecting the total field, as shown below in Fig. 5.

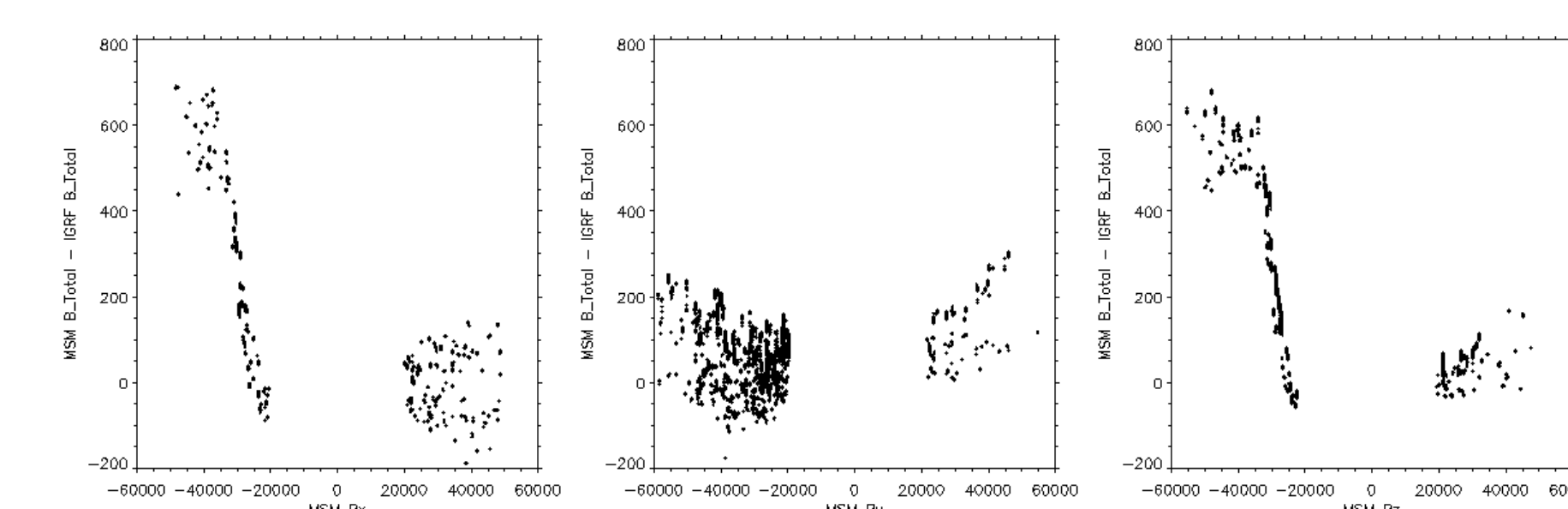


**Fig. 5:** The calibrated MSM total field minus the IGRF model total field, limited to times when each sensor axis is nearly aligned with the magnetic field.

## Data Artifacts

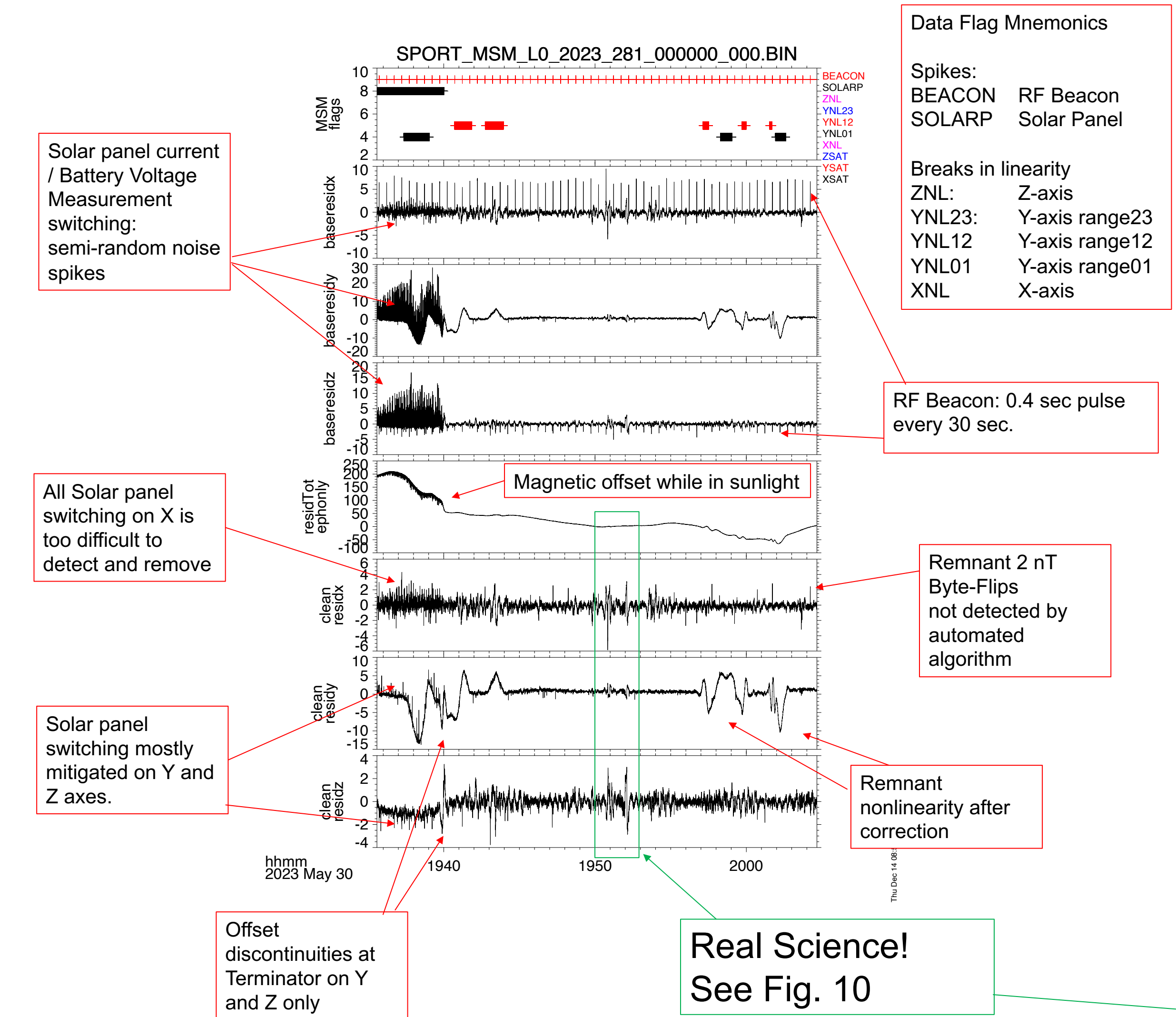


**Fig. 6:** A baseline generated by SSA with 400 components (a 40-sec window) is subtracted from each axis of the MSM data, revealing transient artifacts in the data. Data flags are shown in the top panel, and the next 3 panels show the raw MSM residuals relative to the baseline. The middle panel shows the residual relative to the total IGRF magnetic field. The bottom 3 panels show the residuals on the MSM X, Y, Z components after artifacts have been removed.

### Spacecraft Interference

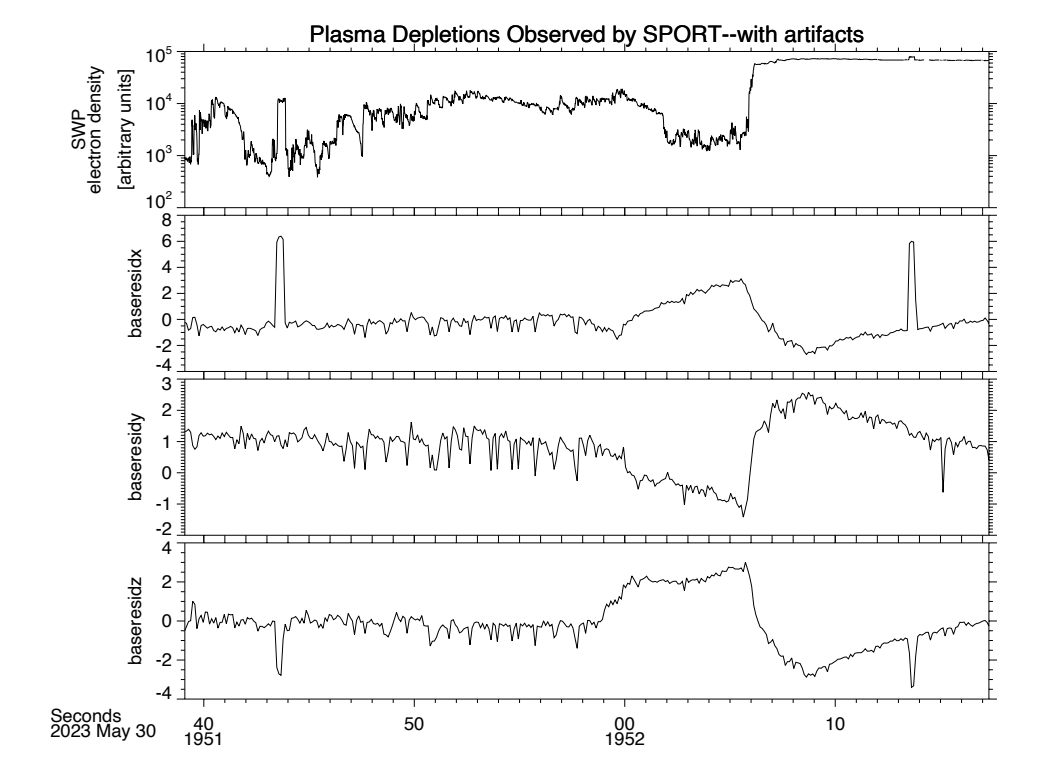


**Fig. 7:** The RF Beacon is seen simultaneously by the SWP Langmuir probe as well as MSM. Easily identifiable as a recurring 6 nT pulse on the X axis, with a corresponding ~2.5 nT pulse on the Z-axis. As each pulse has an identical duration and magnitude, this is potentially correctable. Also note the enhanced noise between 19:51:47 and 19:51:59.

### Telemetry Artifacts: 'Byte-Flips'

Approximately 2% of the SPORT/MSM telemetry bytes are affected by a completely random telemetry error where a telemetry byte value is incremented by 1, e.g. 12->13 or 255->0. When this error affects the 24-bit ADC outputs of the MSM measurement, in the former case this results in a negative spike in pseudo-nT, while in the latter case, it results in a positive spike of 256 times that magnitude! Depending on whether the high-, middle- or low-order byte is affected, these result in random glitches of 508 pseudo-nT or 2 pseudo-nT. If identified, the glitches can be precisely corrected, as the byte value is known. Thus, all 508 p-nT glitches are easily corrected, but the 2 p-nT glitches may escape detection when there are other sources of noise, regardless of origin (see fig. 6). This telemetry anomaly affects all bytes of the MSM telemetry, including the MSM time tags, so ITA developed a flight-software workaround to measure the precise GPS time when an MSM packet is ready, enabling ~5 ms timing accuracy.

## Geophysical Observations

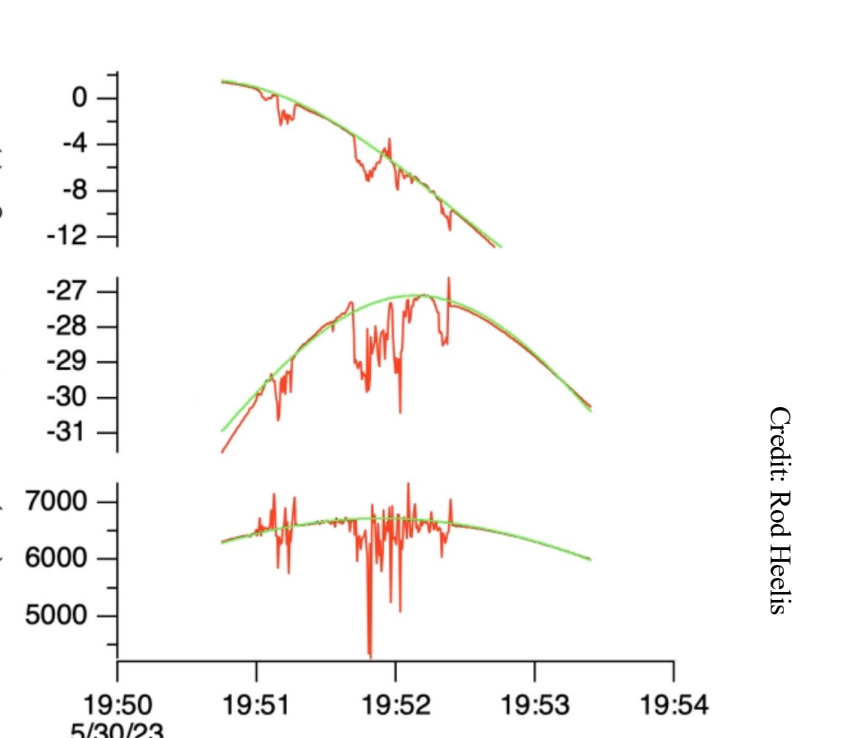
### MSM/IVM Attitude Solution

Although the SPORT bus cannot provide attitude solutions at all times of scientific interest, the attitude of the SC can be calculated from the science observations by the triad method:

The measurements in the S/C frame are

- SC velocity: calculated from the vertical and horizontal ion arrival angles measured by IVM.
- Magnetic field: the calibrated MSM measurement. The reference vectors are
  - SC velocity calculated from the TLE ephemeris, adjusted for the earth co-rotation velocity.
  - IGRF magnetic field at the position of the S/C

**Fig. 8:** IVM ion arrival angles can provide the velocity vector in S/C coordinates when the ram angle is  $< 30^\circ$



## Observed Magnetic Deflections Associated with Plasma Depletions

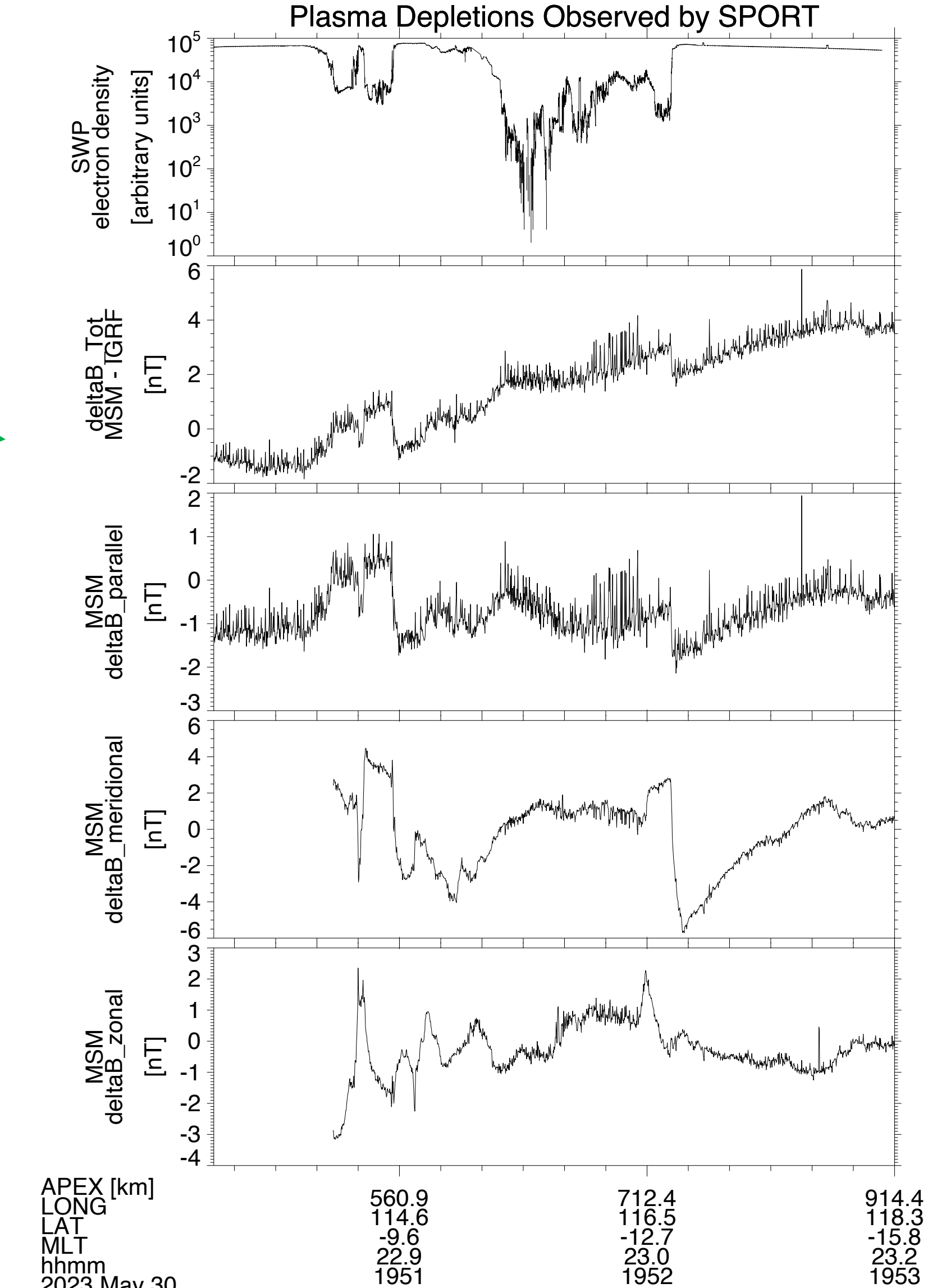


**Fig. 9:** Top panel show the SWP raw ion density measurement. Second panel is the residual of the calibrated MSM total field, as compared to the total IGRF field. In the bottom 3 panels, The  $\Delta\mathbf{B}$  vector is calculated relative to a baseline magnetic field vector generated by summing the lowest 13 components of a 6000-component SSA analysis (10 minute window) of the MSM measurement. The  $\Delta\mathbf{B}$  vector is then rotated into magnetic coordinates defined by the MSM and IVM magnetic field and velocity.

Deflections in the magnetic field are clearly correlated with the structure of the density depletions.

## Discussion

Our calibration and data processing procedures have produced reasonably good results even in the absence of precise attitude knowledge. During the 30 May 2023 plasma depletion events observed simultaneously by the Ion Velocity Meter (IVM) and the Space Weather Probe (SPW) Langmuir probe, MSM observes associated magnetic field perturbations as low as 2 nT which may be associated with the diamagnetic effect, as well as features as large as 5 nT, which may be associated with Alfvén waves. These data are now ready for a rigorous investigation of the physics, as well as a thorough survey of the data set for similar events.

The science data will be distributed from and archived at the INPE Brazilian Monitoring and Study of Space Weather (EMBRACE) regional space-weather forecasting center. The data is planned to be mirrored at the NASA Goddard Space Flight Center (GSFC) Space Physics Data Facility (SPDF).

## References

- Spann, James. "The Scintillation Prediction Observations Research Task (SPORT): An International Science Mission using a CubeSat". 31st Annual AIAA/USU Conference on Small Satellites.
- Stolle, C., Lühr, H., Rother, M., & Balasis, G., "Magnetic signatures of equatorial spread F as observed by the CHAMP satellite", Journal of Geophysical Research: Space Physics, 111(2), 1–13, 2006.